Coupling of the α and β Processes in Poly(ethyl methacrylate) Investigated by Multidimensional NMR

A. S. Kulik,† H. W. Beckham,‡ K. Schmidt-Rohr,§ D. Radloff, U. Pawelzik, C. Boeffel, and H. W. Spiess*

Max-Planck-Institut für Polymerforschung, Postfach 3148, D-55021 Mainz, Germany

Received February 9, 1994; Revised Manuscript Received May 9, 1994®

ABSTRACT: The coupling of the α and β processes in poly(ethyl methacrylate) has been investigated in detail by multidimensional ^{13}C solid-state NMR of the carboxyl moiety. In the glassy state the underlying molecular motion is anisotropic and involves a π flip of the side group coupled to a rocking motion around the local chain axis with a ±20° amplitude. Above the glass transition (T_g) the molecular motion remains highly anisotropic. The geometry of the molecular motion is similar to that in the glass; however, the rocking amplitude increases upon raising the temperature above T_g. This is indicative of a pronounced influence of the α main-chain motion on the β side-group motion which manifests itself by a marked increase of the rocking amplitude to a value of ±50° at 365 K (T_g+ 27 K). It eventually leads to a locally anisotropic uniaxial chain motion at 395 K (T_g + 57 K). This behavior differs significantly from that of other amorphous polymers above T_g where the molecular motions of both the main chain and side groups are isotropic. The averaged correlation times extracted from NMR experiments are in good agreement with data from dielectric relaxation.

I. Introduction

It is well-known that when an amorphous polymer is cooled from the melt it does not crystallize but instead enters the glassy state.[1] The transition to the glassy state is characterized by the glass transition temperature (T_g). Around T_g large changes in the mechanical properties are observed, notably a change in viscosity.[2] These changes can be directly related to the large changes in molecular motions. The diffusional motion and structural changes become highly restricted and slow in contrast to the relatively fast relaxation of the vibrational and librational degrees of freedom.[3] The mean correlation time of the slow chain motion (α process) shows a very strong temperature dependence. Different from the normal Arrhenius-like temperature dependence of an activated process, it is typically described by the Williams–Landel–Ferry (WLF) equation.[4] At T_g structural relaxation times are on the order of minutes. In contrast to the main-chain dynamics, localized motions like those of the side groups do not stop at T_g but persist in the glassy state (β process). The mean correlation time of this localized process shows an Arrhenius-like temperature dependence. The correlation times of both processes usually merge well above T_g.

Among the many experimental techniques employed in probing complex dynamics in the vicinity of T_g, solid-state NMR has proved to be particularly successful.[5] In ^{13}C NMR information on molecular dynamics originates from the anisotropy of the magnetic shielding of the nucleus by the electrons, known as the chemical shift.[6] The dependence of the NMR frequency on the orientation of a given molecular unit relative to the external magnetic field $\mathbf{B}_0$ is given by[6]

$$\omega_0 = \omega_L + \frac{\delta}{2}(3\cos^2\theta - 1 - \eta\sin^2\theta\cos 2\phi) \qquad (1)$$

where ω_L is the Larmor frequency including the isotropic chemical shift, and δ is the strength of the anisotropic coupling. The asymmetry parameter η characterizes the deviation of the chemical-shift tensor (CST) from axial symmetry, and the polar angles θ and ϕ specify the orientation of the magnetic field vector $\mathbf{B}_0$ in the principal axes system of the tensor. The angular dependence of the NMR frequency, shown in eq 1, is used in monitoring molecular dynamics via NMR spectra[7] and relaxation rates.[6] The application of multidimensional NMR to polymers yields both molecular reorientation geometries as well as time scales of motions in amorphous polymers.[5] The α process has been studied extensively with ^2H and ^{13}C exchange NMR;[8-12] however, detailed studies of the β process are more scarce.[13-17]

Recently it was shown by multidimensional solid-state NMR that, in poly(methyl methacrylate) (PMMA), the β process in the glassy state which is active in dielectric and mechanical relaxation[18] is not strictly local.[19] It involves a 180° flip of the carboxyl group accompanied by a main-chain rearrangement characterized as a rotation around the local chain axis ("rocking") with a ±20° amplitude. Moreover, both in PMMA and in poly(ethyl methacrylate) (PEMA), highly anisotropic chain motions were observed above T_g, leading to motionally narrowed NMR spectra. This is indicative of substantial conformational order of the polymethacrylate chains in the melt.[20] The corresponding order parameter as probed by the carboxyl carbon was found to be particularly high for PEMA.

The purpose of the present work is to elucidate the molecular dynamics in PEMA in greater detail. Two-dimensional (2D) and selective-excitation 3D exchange techniques[19] have been applied to study the motion of the side group (β process) in the glass and also above T_g. This study offers the opportunity to compare the molecular dynamics in PEMA and PMMA. The rocking of the main chain associated with the side-group motion in PMMA is due to the asymmetry of the side group, which prevents a fit into the initial environment after a flip.[19] Therefore, it is interesting to check whether the same dynamic process occurs in PEMA, in which the larger side group is conse-

* To whom correspondence should be addressed.
† Present address: Unilever Research Laboratory, Physical and Analytical Sciences, Oliver van Noortlaan 120, NL-3133 AT Vlaardingen, The Netherlands
‡ Present address: School of Textile and Fiber Engineering, Georgia Institute of Technology, Atlanta, GA 30332-0295.
§ Present address: Department of Chemistry, University of California, Berkeley, CA 94720.
® Abstract published in *Advance ACS Abstracts*, July 1, 1994.

0024-9297/94/2227-4746$04.50/0

quently more asymmetric. While the average dielectric relaxation time at each temperature, and therefore the activation energy, for the β relaxation in PMMA and PEMA are the same in the glass,[18] the glass transition temperatures in both compounds differ by about 50 K (PMMA, 390 K; PEMA, 338 K). Thus, the molecular motion in PEMA above T_g where α and β processes operate simultaneously can be compared with that in PMMA at the same temperature where only the β process occurs.

II. Experimental Section

A. NMR Experiments. To facilitate the understanding of the spectra presented below, the relevant features of the experimental techniques employed in this paper are briefly summarized.

Detailed information about geometries of molecular reorientations, as well as time scales of these motions, can be obtained from the 2D exchange experiment.[21] In this experiment, molecular orientation is measured via the NMR frequency (eq 1) before and after a mixing time t_m during which reorientation can take place. The resulting 2D spectrum, $S(\omega_1,\omega_2;t_m)$ represents a two-time distribution function.[8,22] It describes the joint probability density of finding a molecule with frequency ω_1 corresponding to the initial orientation before t_m and frequency ω_2 corresponding to the final orientation after t_m. In the absence of motion, the frequencies ω_1 and ω_2 are the same and the spectral intensity is confined to the diagonal $\omega_1 = \omega_2$. In the case of large-angle reorientation about the same well-defined angle, the 2D spectrum displays characteristic exchange ridges in the form of higher order curves.[5] Random motions or reorientations about ill-defined angles result in a 2D spectrum without sharp contours. Thus, 2D exchange spectra can discriminate between different motional mechanisms.

In this study we are particularly interested in the question of whether the side-group motion in PEMA involves a two-site jump or diffusive motion. This question is best tackled by 3D exchange NMR.[5,23] There, the NMR frequency is probed during three subsequent time periods. During the first evolution period (t_1) the start position is labeled. Reorientation relative to the start position, after the first mixing time (t_{ma}), is probed during the second evolution time (t_2). In the detection period (t_3), after the second mixing time (t_{mb}), the signal is acquired. Thus motions that move the molecular moiety away from its starting orientation during t_{ma} but return it to the same orientation during t_{mb} can be easily detected. For a simple two-site jump this process occurs frequently, whereas for rotational diffusion the return has a very low probability. A convenient way to analyze the 3D exchange spectrum is by individual 2D slices of the cube at a constant frequency ω_1. The information obtained from the 2D slices often is sufficient to distinguish between two-site jumps and diffusive motions. For the former, segments which in the detection period (t_3) have returned to their initial orientations will produce a return-jump ridge at $\omega_3 = \omega_1$ in the (ω_2,ω_3) plane, parallel to the ω_2 axis. Segments that do not exchange during the second mixing time form a diagonal in the (ω_2,ω_3) plane. Therefore, both ridges will have equal intensities and spectral shapes. For diffusive motions no preference exits for return jumps, and the signal in the (ω_2, ω_3) plane will exhibit a diffusive character and the return-jump ridge will be absent. A slice at fixed ω_1 through a 3D spectrum can be measured in a selective-excitation 3D experiment.[19] As described in ref 19, this has advantages in terms of phase-error suppression due to low exchange intensity.

The NMR experiments were carried out on a Bruker MSL-300 spectrometer operating at a ^{13}C resonance frequency of 75.47 MHz. All spectra were recorded with cross polarization[24] applying a contact time of 2 ms in a variable-temperature double-resonance probe. The ^1H 90° pulse was 4.5 μs. The probe temperature was controlled with standard Bruker equipment.

The 2D spectra were taken with 30–64 t_1 increments of 32 μs. Typically about 500 scans were averaged. In the selective 3D exchange experiments, a narrow band of frequencies was selected with the SELDOM technique.[25] The selective 3D spectra were recorded with 32 t_2 increments, and 1720 scans were averaged. The mixing time in both mixing periods was 50 ms.

Fourier transformation of the data, data analysis, and all simulations were performed on a VAX computer system. For a comprehensive description of the spectral simulations we refer to ref 5.

B. Preparation of ^{13}C-Enriched Monomer. The synthesis of the ^{13}C-labeled monomer was performed in a two-step reaction. In the first step acetone cyanohydrin was prepared by the reaction of acetone with ^{13}C-labeled sodium cyanide (Cambridge Isotopes) in the presence of 40% sulfuric acid at temperatures between 10 and 20 °C.[26] The reaction product was isolated via extraction with diethyl ether. This process was followed by vacuum distillation. (Bp: 66–68 °C/20 mbar.) The yield was 68%.

The monomer, ethyl methacrylate,[27] was obtained from the acetone cyanohydrin after elimination of H_2O in the presence of fuming sulfuric acid at 60 °C, yielding methacrylonitrile. In order to avoid polymerization, hydroquinone was added as an inhibitor. The saponification of the nitrile and the esterification were performed without isolation of the methacrylonitrile. An ethanol/water mixture was added at a bath temperature of 110 °C (reaction temperature 90 °C). The mixture was then held at that temperature and stirred for 708 h. The monomer was isolated by steam distillation followed by successive extractions with diethyl ether and finally by fractional distillation. (Main fraction bp: 70 °C/900 mbar). The yield of the ester was 25%.

C. Polymerization. The polymer was obtained by free-radical polymerization in toluene at 60 °C with 8.5 mol % azobis(isobutyronitrile) as initiator. The polymer was then precipitated in cold methanol for purification. The yield was 70%. In the polymerization only 20% of the labeled ethyl methacrylate was used. The remaining 80% of the monomer was taken from a commercial source (Merck) and distilled prior to the polymerization. This concentration of 20% labeled material was chosen in order to avoid homonuclear dipolar broadening of the ^{13}C spectra and to prevent exchange by spin diffusion.

The molecular weight was characterized by GPC (calibrated with PMMA standards): M_w = 120 000 and M_w/M_n = 2.2. Analysis of the ^1H spectra of PEMA dissolved in $CDCl_3$ revealed the following distribution of triads: 11% isotactic (mm), 58% syndiotactic (rr), and 31% heterotactic (rm). The glass transition temperature measured with DSC was 338 K. Prior to measurement, the NMR sample was melt pressed at T = 363 K (25 K above T_g) for 30 min.

III. Results and Discussion

A. One-Dimensional Spectra. As mentioned in our previous study of PMMA,[19] the signal-to-noise ratios in the natural abundance ^{13}C NMR spectra are too low to analyze the details of the molecular reorientation with multidimensional experiments. Therefore, similar to our previous investigations of PMMA, our study of PEMA was carried out on a sample in which the carboxyl carbon was ^{13}C enriched by 20%. Figure 1 shows ^{13}C NMR spectra of the carboxyl carbon in PEMA as a function of temperature. Only the carboxyl region is shown which does not overlap with the signals of the aliphatic carbons. This enables investigation of the side-group motion through analysis of the line shape of the carboxyl carbon. The spectrum recorded at 295 K clearly shows terminating edges and a peak corresponding to the principal values of the asymmetric chemical-shift tensor (CST) (ω_{11} = 268 ppm, ω_{22} = 150 ppm, ω_{33} = 113 ppm). As the temperature is raised, pronounced line-shape changes are observed, indicating large-amplitude motions with rates exceeding the width of the powder spectrum, that is, above 10 kHz. At 395 K the anisotropic chain motion leads to the line shape of a motionally averaged axially symmetric tensor, from which the order parameter of the conformational order can be determined.[20]

To understand the results presented here, knowledge of the orientation of the principal axes system of the CST relative to the chain axis is required. In earlier measurements of the ^{13}C CST of the carboxyl carbon[28] it was

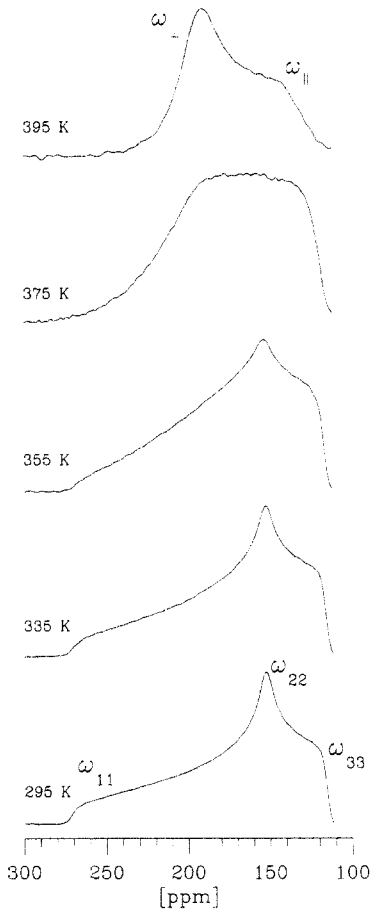

Figure 1. Experimental ^{13}C NMR spectra of the carboxyl carbon in PEMA as a function of temperature.

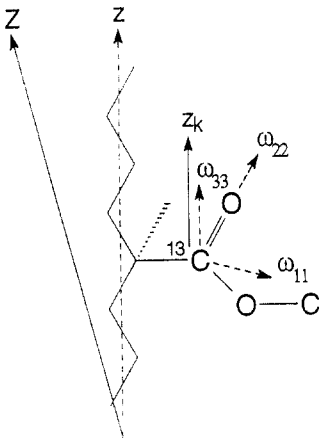

Figure 2. Orientation of the principal axes system of the chemical-shift tensor of the carboxyl carbon relative to the chain axis in PEMA and PMMA. The direction of the extended polymer chain is denoted by Z, the local chain axis by z, and the ω_{33} axis of the CST of the carboxyl carbon by z_k. Note that z and z_k are approximately parallel.

determined that the most shielded component of the shift tensor (ω_{33}) is perpendicular to the OCO^- plane, with the two others being in the plane. This means that the ω_{33} direction is parallel to the chain axis, with the other two principle tensor elements being in the plane of the side group as depicted in Figure 2.[19,20] This assignment has recently been confirmed in an investigation of oriented PMMA.[29]

B. Molecular Motion in the Glassy State. In principle, it is possible to simulate measured 1D spectra (Figure 1) and extract geometric information out of these spectra. However, this would require extensive simulation of the spectra with many adjustable parameters; a fit of the experimental line shape would hardly be unique.[19] Two-dimensional exchange NMR is far superior to 1D techniques for studying the geometry of molecular reorientations and therefore is used in the present study. Figure 3 shows the 2D spectrum at 298 K for t_m = 500 ms. The exchange pattern resembles the spectrum of glassy PMMA,[19] where a coupled motion of the side group and the backbone was found. The exchange signal at ω_{33} is low as compared with exchange between ω_{22} and ω_{11}. This suggests that the principal axis ω_{33} remains invariant in the motional process. This would result by either a rotation about this axis or by π flips of the side group which leave the ω_{33} frequency unchanged due to the nature of the interaction (cf. eq 1). The absence of elliptical ridges in the 2D spectrum excludes π flips as the only motional mechanism. The elliptical ridges would appear between ω_{22} and ω_{11}. As was pointed out previously,[19] restricted rotation around the ω_{33} axis parallel to the local chain axis is an effective mechanism for broadening elliptical ridges, while producing no exchange at ω_{33}. Thus, as in PMMA the exchange pattern in Figure 3 can only be explained by assuming that π flips of the side group are accompanied by a reorientation of the main chain.

Although the spectrum in Figure 3 was recorded for a mixing time that was about 5 times longer than the correlation time of the β process, as determined by NMR (see below), the off-diagonal intensity represents only about 20% of the total. For a jump between two sites, 50% of the intensity is off-diagonal. This means that only ≈40% of the side groups participate in the motion on the time scale of the experiment, while ≈60% remain immobile, presumably due to constraints in the local environment. This is indicative of a heterogeneous distribution of correlation times. The simulated spectrum, based on the model proposed above is shown in Figure 3. This calculation was performed for a rocking amplitude of ±20° coupled to the π flips and assuming that 40% of the segments participate in the motion. The agreement with the experimental spectrum is rather good. We conclude that in the glassy state of PEMA π flips of the side group are coupled to a restricted rotation around the local chain axis of the main chain. Our results show that the geometry of the molecular motion in glassy PEMA is the same as that in glassy PMMA. However, the number of side groups participating in the molecular motion is somewhat smaller in PEMA than in PMMA. The NMR results for both compounds can be directly compared since experiments were performed at the same reduced temperature $T^* = T/T_g = 0.88$. It was found that in PMMA ≈50% of the units were trapped in local environments, while in PEMA ≈60% remained immobile. Also, experiments performed on PMMA at 268 K revealed that the number of immobile units remain ≈50% on a time scale about 5 times longer than the correlation time of the β process. Presumably, lower exchange intensity in PEMA is due to the larger ethyl side group. This is consistent with dielectric relaxation results, where it was found[30] that the ϵ'' amplitude in PEMA is lower than that in PMMA due to the ratio between the strength of the dipole moment and the bulkiness of the side group.

The similarity between the side-group motion in the glassy state of PEMA and PMMA was further checked by a series of measurements along the same lines as described for PMMA in ref 19. First, exchange due to spin diffusion was ruled out when a 2D spectrum recorded at 235 K and t_m = 500 ms contained no exchange intensity, thereby signifying a strong temperature dependence for the

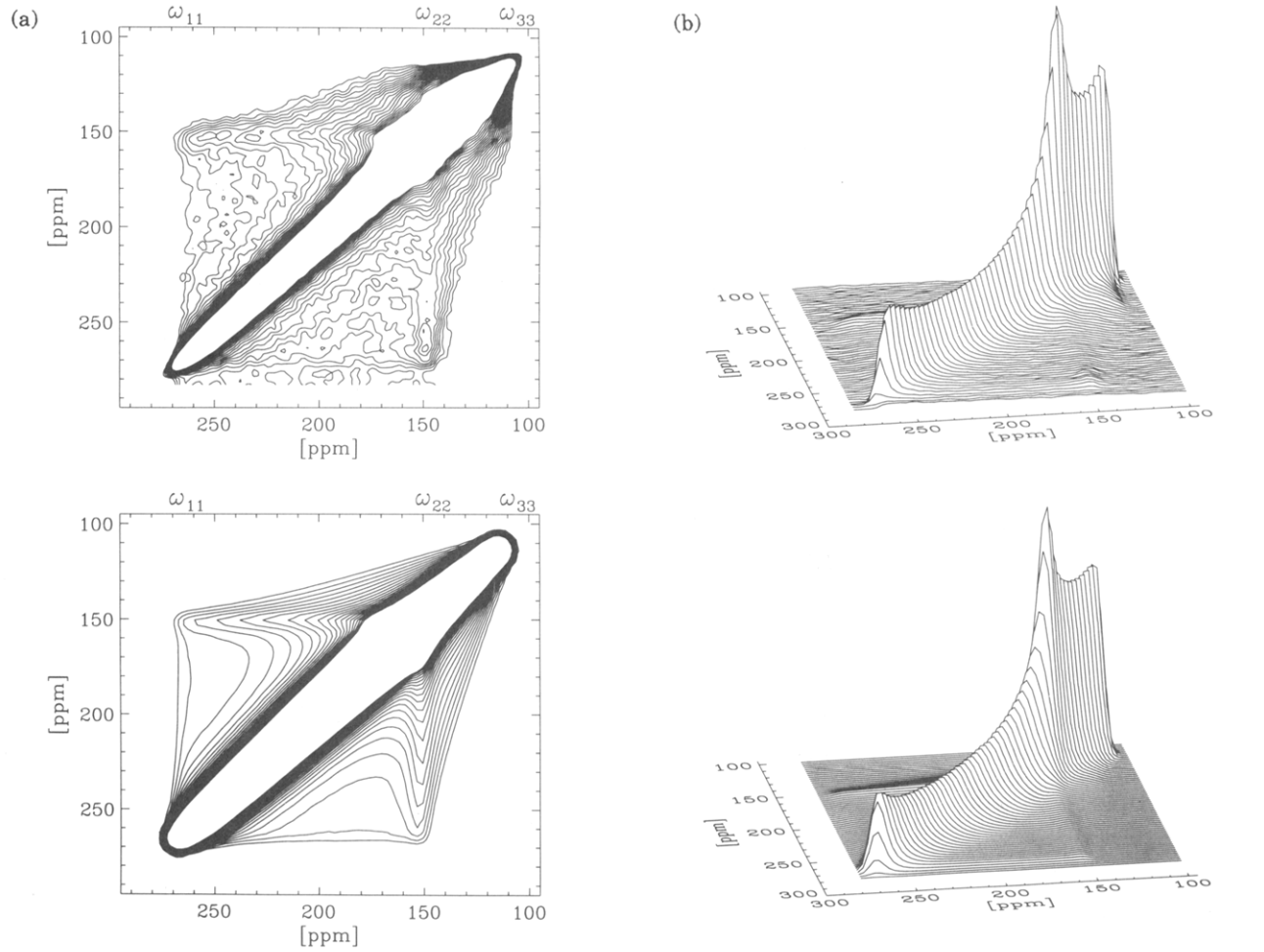

Figure 3. 2D exchange ^{13}C NMR spectrum of the carboxyl carbon in PEMA taken at 298 K, with t_m = 500 ms, and simulation. (a) Contour plots. The contour lines are linear between 0.5% and 5% of the maximum. Upper plot: experimental. Lower plot: simulation. (b) Stacked plots. Upper plot: experimental. Lower plot: simulation.

exchange process. By the selective 3D exchange NMR experiments the existence of back-rotations due to π flips was checked. Finally, *m*ultiple *e*xchange and *s*elective *s*aturation for *a*nalysis of the *g*rowth of *e*xchange (MESSAGE) experiments were employed to probe the heterogeneous distribution of correlation times.

C. Molecular Motion above T_g. As mentioned in the Introduction, the side-group motion in PEMA can be studied by multidimensional NMR even above T_g. Figure 4 shows 2D exchange spectra of PMMA and PEMA recorded at the same temperature of 355 K and the same mixing time of 500 ms. Both spectra are plotted with the same contour levels. At this temperature PMMA is in the glassy state, while PEMA is in the melt, 17 K above T_g. A mixing time of 500 ms corresponds to the full exchange limit, since the mean correlation times are at least an order of magnitude shorter in both materials (vide infra). The exchange intensity in the PEMA spectrum is much larger than in that of PMMA, but the exchange patterns for both are quite similar. In fact, they resemble the exchange pattern of PEMA at 298 K shown in Figure 3, however, with higher exchange intensity. In both spectra the exchange signal at ω_{33} is lower than that of exchange between ω_{22} and ω_{11}. The spectra were integrated to determine the percentage of side groups participating in the motion. Apparently in PEMA ≈85% of the side groups take part in the motion, while in PMMA this fraction is only ≈65%. The lower number of mobile units in PMMA is ascribed to the fact that this polymer is in the glassy state in contrast to PEMA at this temperature. We note that, although PEMA is above T_g, ≈15% of the units still remain trapped in their local environments on the time scale of the experiment. This is presumably due to the bulkier side group which requires a substantial volume for reorientation. Thus, in the molten state of PEMA the geometry of the side-group motion is only slightly modified, but the number of units involved in this motion is drastically increased. The similarity of the exchange patterns and the fact that the PMMA in the glassy state exhibits anisotropic motion suggest that in PEMA even above T_g the molecular motion is anisotropic, with the molecular geometry similar to that in the glass. This behavior differs significantly from that of other amorphous polymers like polystyrene[31] and poly(vinyl acetate),[5,12] where the molecular motion of the side groups above T_g is isotopic and reflects the ill-defined reorientations of the main chain.

The nature of the side-group motion above T_g can be further checked by 3D exchange NMR. As mentioned in section II.A and explained in detail elsewhere,[5,19] a suitably chosen 2D slice of a 3D spectrum can prove a two-site jump process. Figure 5 shows a 2D slice (ω_2, ω_3) of the 3D spectrum at constant ω_1. The slice was recorded in a selective-excitation 3D experiment[19] at 345 K, 8 K above T_g with mixing times $t_{ma} = t_{mb}$ = 50 ms. This is comparable to the mean correlation time of the side-group motion, however, much shorter than the mean correlation time of the α process (vide infra). The ω_1 frequency was selected near the ω_{11} edge of the carboxyl carbon powder pattern. The two well-resolved ridges along the $\omega_2 = \omega_3$ diagonal,

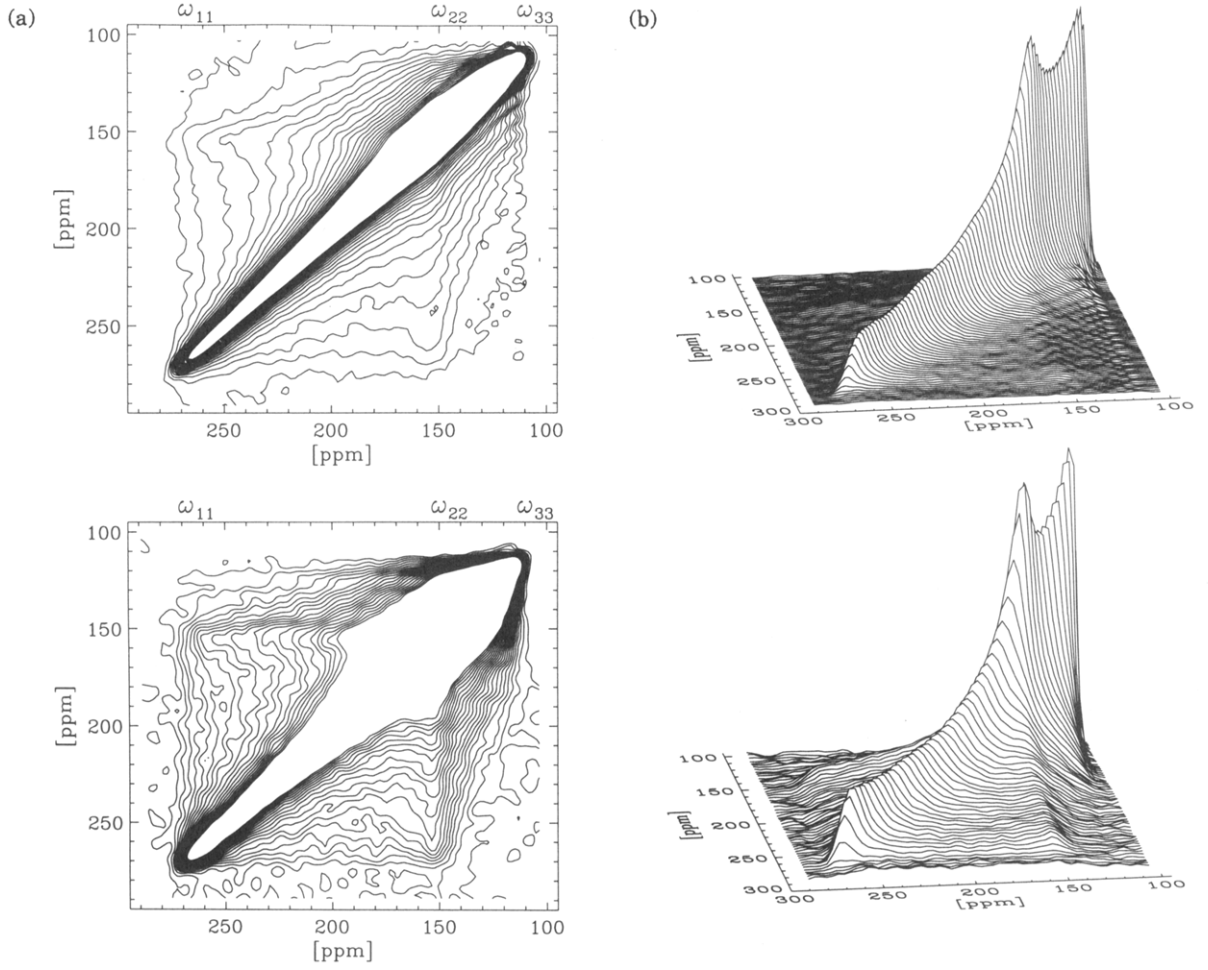

Figure 4. 2D exchange ^{13}C NMR spectrum of the carboxyl carbon in PMMA and PEMA at 355 K, taken with t_m = 500 ms. (a) Contour plots. The contour lines are linear between 0.5% and 15% of the maximum. Upper plot: PMMA. Lower plot: PEMA. (b) Stacked plots. Upper plot: PMMA. Lower plot: PEMA.

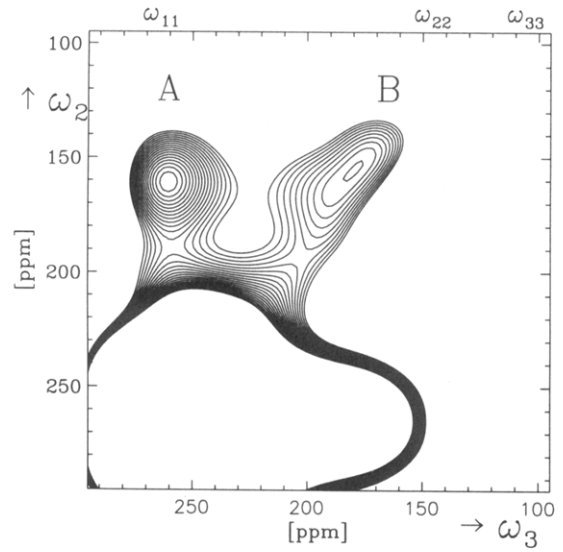

Figure 5. Selective-excitation 3D NMR exchange spectrum of the carboxyl carbon in PEMA (T = 345 K, t_{ma} = t_{mb} = 50 ms). The ω_1 frequency was selected near the ω_1 edge of the carboxyl powder spectrum. The contour lines in the (ω_2, ω_3) plane are linear between 1% and 3%. The return-jump ridge is labeled A; the diagonal is labeled B.

labeled B, and along the $\omega_1 = \omega_3$ line, labeled A, prove that, despite the diffusive appearance of the 2D exchange patterns in Figures 3 and 4, the reorientation must occur between two relatively well-defined potential energy minima. This holds not only below T_g but also above it. This observation is remarkable considering the substantial changes in local environments which should take place on increasing temperature above T_g. Therefore, an increase in the amplitude of the main-chain rocking motion is expected. Indeed, in order to fit the experimental 2D exchange spectrum of PEMA, shown in Figure 4, the rocking amplitude had to be increased to ±40° (cf. Figure 6). The simulation also includes the presence of 15% rigid side groups (see above).

It was experimentally possible to record the 2D exchange spectrum with t_m = 5 ms at 365 K, which is 27 K above T_g (Figure 7). As compared with the spectrum recorded at 355 K, not only is the time scale of the motion reduced but also significant changes of the line shape along the diagonal and the much higher exchange intensity are observed. The highest intensity now is the peak at ω_{33}, while the intensities at ω_{22} and ω_{11} are reduced.

The integrated exchange intensity is ≈100%. Apparently all segments participate in the motion on the time scale of 5 ms.

The question whether the side-group motion is anisotropic or isotropic at 365 K can be easily clarified by inspection of the simulated spectrum for isotropic diffusion presented in Figure 8. This motional model is consistent with previous ^{13}C NMR studies of molecular motion in amorphous polymers above T_g.[5,12] However, it differs substantially from the experimental spectrum at 365 K. In particular, the line shape on the diagonal is different. The highest peak appears around ω_{22}, in stark contrast

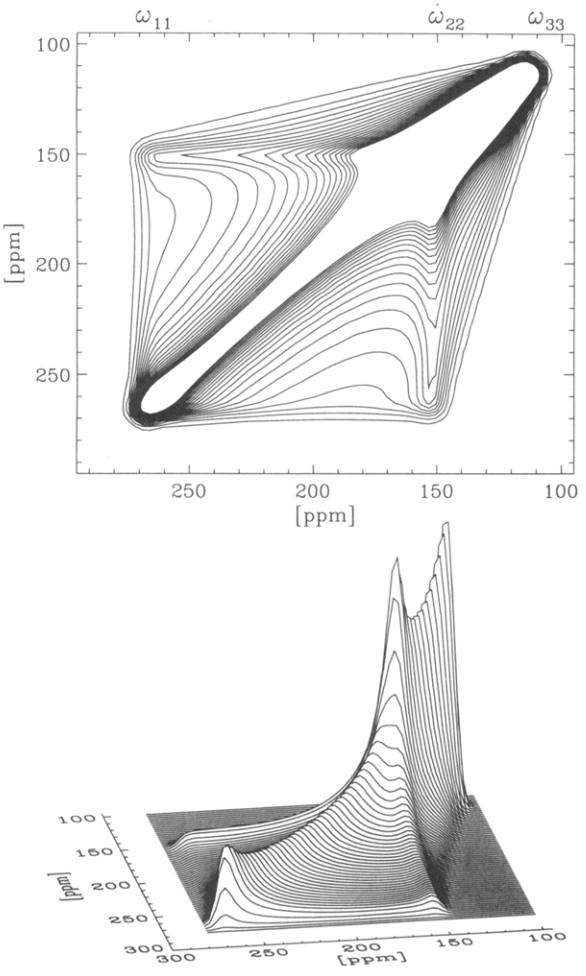

Figure 6. Simulation of the spectrum at 355 K for PEMA. Upper plot: contour plot. The contour lines are linear between 0.5% and 15% of the maximum. Lower plot: stacked plot.

to the experimental spectrum where the maximum is close to ω_{33}. The exchange pattern is also different, showing the exchange intensity spread out over the whole 2D plane, while in the experimental spectrum the exchange pattern is confined to a markedly smaller region.

The details of the anisotropic motion can be further elucidated by simulation of the 2D spectrum. Since the line shape on the diagonal in the experimental spectrum is significantly affected by molecular motion (see Figure 1), this should be taken into account in the simulation. There are several ways to do this, by complete and approximate methods. The first is mathematically and numerically demanding. It requires introduction of frequency changes in the calculation of the signal in the evolution and the detection period. An example of such a treatment was used in the analysis of 2D exchange spectra in ^{2}H NMR of amorphous polymers. A full description of the theory involved can be found in a series of papers published recently.[9,10] We did not attempt to follow this approach here due to the complexity of the molecular motions in PEMA, involving anisotropic side-group and main-chain motions of different amplitudes. Since at this point only the *main features* of this complex dynamics are of interest, a slightly crude but numerically facile approximation was used. The 2D exchange spectrum was simulated as usual for the slow-motion limit $S_0(\omega_1,\omega_2)$. Each point was then weighed by the probability $P(\omega)$ that the corresponding frequencies occur in the 1D NMR line shape, or equivalently in the projection of the 2D spectrum onto the ω_1 or ω_2 axis

$$S_1(\omega_1,\omega_2) = S_0(\omega_1,\omega_2)\frac{P_1(\omega_1)\,P_1(\omega_2)}{P_0(\omega_1)\,P_0(\omega_2)} \qquad (2)$$

where P_1 and P_0 are the projections of the experimental and calculated spectra, respectively. P_0 is taken from the powder spectrum of the rigid solid (see Figure 1; 295 K), and P_1 is taken from the experimental 1D spectrum at 365 K, not shown in Figure 1. Such a calculation was performed for a rocking amplitude of ±50° coupled to the π flips and assuming that all segments participate in the motion. The result, plotted in Figure 7, shows remarkable agreement with the experimental spectrum.

The results of our analysis of the complex dynamics of the side group in PEMA are summarized in Figure 9. Because the ω_{22} and ω_{33} values of the static CST are quite similar for the carboxyl carbon and because the ω_{33} axis is hardly involved in the exchange process, the exchange intensity mainly reflects the reorientational angle distribution[5,8] of the ω_{11} axis in the plane perpendicular to the local chain z_k (see Figure 2). This quantity, as determined from the fits of the experimental NMR spectra, is plotted for the different temperatures in Figure 9. In the glassy state at 298 K, the side-group motion involves a π flip coupled to a rocking motion around the local chain axis with an amplitude of ±20°. Only 40% of the side groups are involved in this process. Above T_g, at 355 and 365 K the coupling of the β side-group and α main-chain motions increases, which manifests itself by a pronounced increase in the rocking amplitude with values of ±40° at 355 K and ±50° at 365 K. This eventually leads to the highly anisotropic chain motion well above T_g reported earlier,[20] where the rocking motion about the local chain axis remains faster by more than 2 orders of magnitude than the rotation of the chain axis itself. This uniaxial motion is evidenced by the motionally narrowed spectrum at 395 K (see Figure 1), which exhibits the typical line shape of an axially symmetric CST and indicates substantial conformational order in the molten state.

D. Temperature Dependence of Correlation Times for the α and β Processes. The analysis of the 2D spectra also yields the correlation times of the side-group motion which can be compared with the results for the dynamics in PEMA obtained by other techniques. Figure 10 shows average correlation times for the α and β processes determined by dielectric relaxation[30] and photon correlation spectroscopy (PCS).[32] They are compared with correlation times extracted from our NMR experiments. As can be seen from Figure 10, the correlation times found with PCS exhibit a significant non-Arrhenius temperature dependence, typical for α processes. By using high pressure, separation of α and β processes was achieved.[33] This technique probes density fluctuations of the local dielectric constant which cause scattering of light, providing averages over macroscopic volumes. Dielectric relaxation probes changes of the dipole moment which originates in PEMA from the carboxy group. Therefore, it is particularly sensitive to the motion of the side group. Since the dipole moment is well localized and the dimensions of the side group are rather small, dielectric relaxation also probes the β process above T_g; apparently this process remains rather insensitive to the motion of the backbone. In the present NMR study, the molecular motion of the carboxyl carbon was monitored. The NMR signal is localized at the same position as the dipole moment. Therefore, the correlation times obtained with NMR and dielectric relaxation agree rather well.

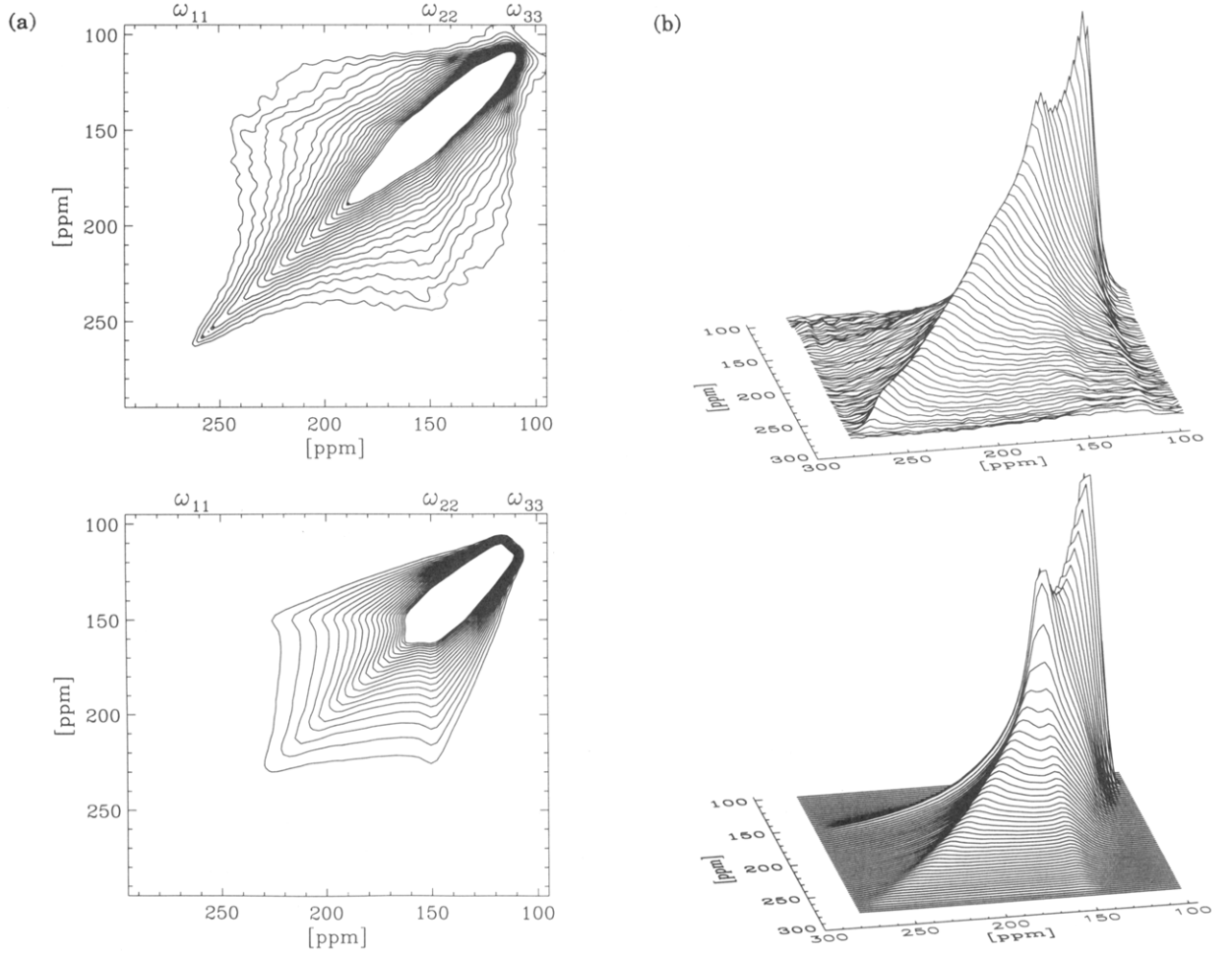

Figure 7. 2D exchange ^{13}C NMR spectrum of the carboxyl carbon in PEMA taken at 365 K, with t_m = 5 ms, and simulation. (a) Contour plots. The contour lines are linear between 5% and 40% of the maximum. Upper plot: experimental. Lower plot: simulation. (b) Stacked plots. Upper plot: experimental. Lower plot: simulation.

The activation energy for the side-group motion in the glassy state, $\Delta E \approx 72$ kJ/mol, agrees well with that deduced from dielectric relaxation,[30] $\Delta E \approx 76$ kJ/mol. However, dielectric relaxation does not yield clear-cut information about the geometry of the motion. Thus, it cannot detect the coupling of the side-group and the main-chain motions detected here by multidimensional NMR. Because of this coupling, activation energies were not extracted from the correlation times above T_g. Likewise, the motional mechanism of the main chain (α process) cannot be inferred from the PCS data. Since NMR shows that the chain motion is highly anisotropic, it is interesting to compare the PCS data with the correlation times of the rocking motion. At temperatures above approximately 370 K, where the rocking motion amplitudes are above ±50°, its correlation time is probed by PCS. However, as shown recently,[20] substantial conformational order exists even at 395 K, where extended regions of the chain relax only on a time scale which is longer than the correlation times of the rocking motion by at least 2 orders of magnitude. Close to T_g, where the rocking amplitude is markedly reduced to ±20°, this faster motion is apparently not detected by PCS and correlation times of the α and the β processes are well separated.

As mentioned in the Introduction, in amorphous polymers exhibiting both an α and a β process, it is known that at temperatures somewhat above T_g the β process merges with the α process.[34,35] Recently Rössler showed[36] that in many supercooled liquids exhibiting both an α and a β process the coalescence of both processes is around $T_g/T = 0.85$. Apparently this finding is not restricted to supercooled liquids. The merging of the α and β processes around $T_g/T = 0.85$ was reported recently in amorphous polystyrene.[37] As can be seen for PEMA in Figure 10, merging of the α and β processes also appears around 400 K, consistent with the reduced temperature T_g/T of 0.85. It is noteworthy that a similar result was reported in a recent study of reorientational dynamics of Disperse red 1 doped at 2 wt % in PEMA.[38] Likewise, unusual mechanical behavior ascribed to the coupling of α and β processes has been reported recently by Donth and coworkers[39,40] for poly(*n*-butyl methacrylate) which has an even bulkier side group. In view of the anisotropy of the chain motion in the methacrylates detected by NMR, it will be interesting to probe the slow dynamics of the main chain directly by multidimensional ^2H NMR of chain-labeled PEMA. Work along these lines is in progress.

E. Nature of the Motion. Our analysis of ^{13}C NMR data shows that motion of the side group in PEMA is highly restricted not only in the glass but also above T_g. On a time scale larger than the mean correlation time, a considerable number of segments are trapped in the structure. Raising the temperature increases the fraction of units participating in the motion. These changes can be estimated from the off-diagonal intensity in the 2D spectra. The constraints to the motion are caused by the packing of the chains and the interaction between neighboring chains. Figure 11 shows the fractions of mobile units that participate in the flip process as obtained from the analysis of the spectra. A gradual change as a

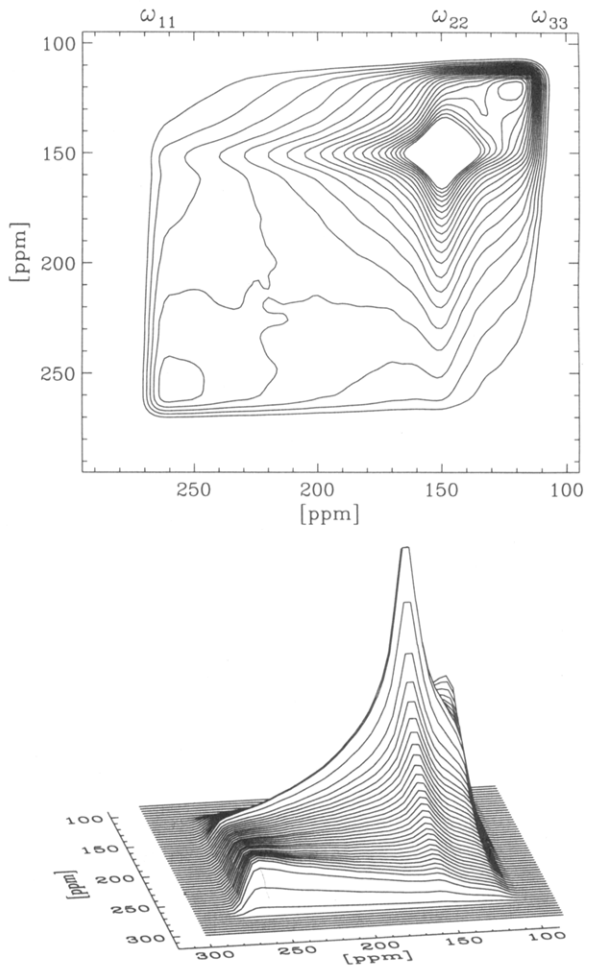

Figure 8. Simulation of the spectrum for isotropic rotational diffusion. Upper plot: contour plot. The contour lines are linear between 5% and 40% of the maximum. Lower plot: stacked plot.

function of temperature is observed. Again, our results are consistent with those of dielectric relaxation.[30] There, it was found that the ϵ'' amplitude increases with temperature. This roughly corresponds to larger fractions participating in the molecular motion. It is highly remarkable that ≈15% of the segments still appear to be arrested in the structure 18 K above T_g. Thus, the packing restrictions on the side-group motion in PEMA are also substantial above T_g. Presumably, this is due to the anisotropic nature of the molecular motion involving a bulky group.

Due to the asymmetry of the side group, its motion occurs between energetically inequivalent sites. From the data presented in Figure 11, an attempt to obtain the energy difference δE between two relatively well-defined potential energy minima has been made (see above). Populations of units in those minima are described by $p_1 = p_0 \exp(-\delta E/RT)$. From the fractions of mobile units that participate in the motion at different temperatures, the energy difference between those two energy minima was estimated to be about 13 kJ/mol. As expected, this value is much lower than that of the energy barrier which separates these two energy minima, namely, 72 kJ/mol (see section III.D).

F. Conclusions. Employing multidimensional ^{13}C NMR experiments, the molecular motion of the side group in PEMA was elucidated in detail, below as well as above T_g. In the glassy state the molecular motion is anisotropic. It consists of π flips of the side group accompanied by the rotation of the backbone around the local chain axis by

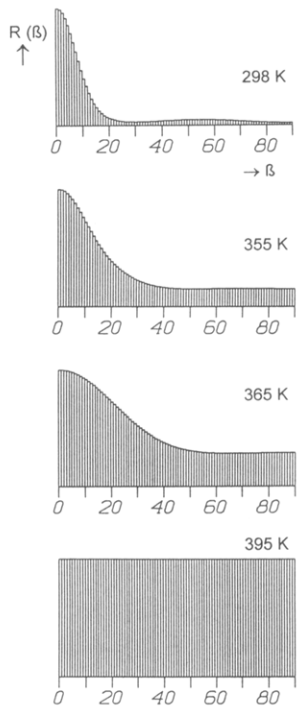

Figure 9. Reorientational angle distribution for the ω_{11} axis of the chemical-shift tensor of the carboxyl carbon in the plane perpendicular to the local chain axis as obtained from the fits of the experimental spectra.

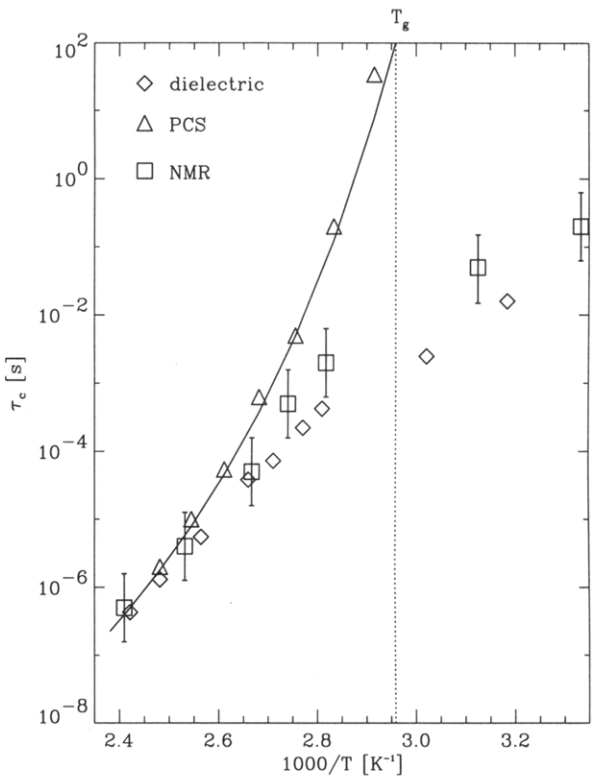

Figure 10. Temperature dependence of the correlation time for the molecular motion in PEMA obtained with various experimental techniques: (□) NMR, present study; (▲) photon correlation spectroscopy; (◇) dielectric relaxation. ◇ and ▲ are results reported in refs 30 and 32, respectively.

±20°. The molecular motion remains highly anisotropic even above T_g. The geometry of the molecular motion is similar to that in the glass; however, the rocking amplitude increases with increasing temperature above T_g. At 365 K (T_g + 27 K), it is about ±50°. This indicates a pronounced coupling between the side-group and the main-

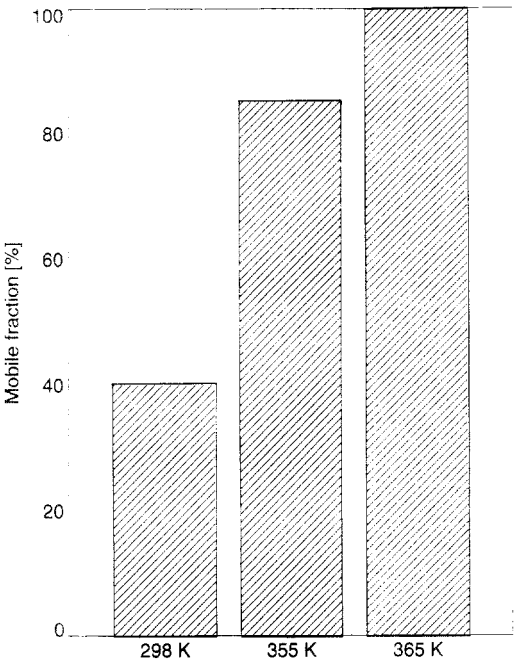

Figure 11. Mobile fractions in PEMA as obtained from the integration of experimental spectra as a function of temperature.

chain motions, that is, between the β and the α processes. The anisotropic molecular motion above T_g is contrary to earlier findings in amorphous polymers where molecular motion is dominated by ill-defined jumps. This is indicative of substantial conformational order of the methacrylate backbone in PEMA. The mean correlation times vary from milliseconds to microseconds and coincide with the data from dielectric relaxation.

Acknowledgment. A.S.K. benefitted from discussions with Dr. Tadeusz Pakula and acknowledges a stipend from the Max Planck Society. H.W.B. is a recipient of an Alexander von Humboldt fellowship. Financial support from the Deutsche Forschungsgemeinschaft (SFB 262) is gratefully acknowledged.

References and Notes

(1) Young, R. J.; Lovell, P. A. *Introduction to Polymers*, Chapman and Hall: London, 1991.
(2) Ferry, J. D. *Viscoelastic Properties of Polymers*; Wiley: New York, 1980.
(3) Jäckle, J. *Rep. Prog. Phys.* **1986**, *49*, 171.
(4) Williams, M. L.; Landel, R. F.; Ferry, J. D. *J. Am. Chem. Soc.* **1955**, *77*, 3701.
(5) Schmidt-Rohr, K.; Spiess, H. W. *Multidimensional NMR and Polymers*; Academic Press: New York, 1994.
(6) Abragam, A. *The Principles of Nuclear Magnetism*; Clarendon: Oxford, U.K., 1961.
(7) Spiess, H. W. *Chem. Rev.* **1991**, *91*, 1321.
(8) Wefing, S.; Kaufmann, S.; Spiess, H. W. *J. Chem. Phys.* **1988**, *89*, 1234.
(9) Kaufman, S.; Wefing, S.; Schaefer, D.; Spiess, H. W. *J. Chem. Phys.* **1990**, *93*, 197.
(10) Schaefer, D.; Spiess, H. W.; *J. Chem. Phys.* **1992**, *97*, 7944.
(11) Schaefer, D.; Spiess, H. W.; Suter, U. W.; Fleming, W. W. *Macromolecules* **1990**, *23*, 3431.
(12) Schmidt-Rohr, K.; Spiess, H. W. *Phys. Rev. Lett.* **1991**, *66*, 3020.
(13) Schaefer, J.; Stejskal, E. O.; McKay, R. A.; Dixon, W. T. *Macromolecules* **1984**, *17*, 1749.
(14) Inglefield, P. T.; Amici, R. M.; O'Gara, J. F.; Hung, C.-C.; Jones, A. A. *Macromolecules* **1983**, *16*, 1552.
(15) O'Gara, J. F.; Jones, A. A.; Hung, C.-C.; Inglefield, P. T. *Macromolecules* **1985**, *18*, 1117.
(16) Hansen, M. T.; Boeffel, C.; Spiess, H. W. *Colloid Polym. Sci.* **1993**, *271*, 446.
(17) Kulik, A. S.; Prins, K. O. *Polymer* **1993**, *34*, 4635.
(18) McCrum, N. G.; Read, B. E.; Williams, G. *Anelastic and Dielectric Effects in Polymer Solids*; Wiley: London, 1967.
(19) Schmidt-Rohr, K.; Kulik, A. S.; Beckham, H. W.; Ohlemacher, A.; Pawelzik, U.; Boeffel, C.; Spiess, H. W. *Macromolecules*, previous paper in this issue.
(20) Kulik, A. S.; Radloff, D.; Spiess, H. W. *Macromolecules* **1994**, *27*, 3111.
(21) Ernst, R. R.; Bodenhausen, G.; Wokaun, A. *Principles of Nuclear Magnetic Resonance in One and Two Dimensions*; Clarendon: Oxford, U.K., 1987.
(22) Wefing, S.; Spiess, H. W. *J. Chem. Phys.* **1988**, *89*, 1219.
(23) Spiess, H. W.; Schmidt-Rohr, K. *Polym. Prepr. (Am. Chem. Soc., Div. Polym. Chem.)* **1992**, *33*, 68.
(24) Pines, A.; Gibby, M. G.; Waugh, J. S. *J. Chem. Phys.* **1973**, *59*, 569.
(25) Tekely, P.; Brondeau, J.; Elbayed, K.; Retournard, A.; Canet, D. *J. Magn. Reson.* **1988**, *80*, 509.
(26) Cox, R. F. B.; Stormant, R. T. *Organic Syntheses*; Wiley: New York, 1943; Collect. Vol. II, p 7.
(27) Naarmann, H., personal communication.
(28) Pines, A.; Abrahamson, E. *J. Chem. Phys.* **1974**, *60*, 5130.
(29) Kulik, A. S.; Spiess, H. W. *Makromol. Chem.* **1994**, *195*, 1755.
(30) Ishida, Y.; Yamafuji, K. *Kolloid Z.* **1961**, *177*, 97.
(31) Spiess, H. W. *Colloid Polym. Sci.* **1983**, *261*, 193.
(32) Patterson, G. D.; Stevens, J. R.; Lindsey, C. P. *J. Macromol. Sci., Phys.* **1980**, *18*, 641.
(33) Fytas, G.; Patkowsky, A.; Meier, G.; Dorfmüller, Th. *J. Chem. Phys.* **1984**, *80*, 2214.
(34) Williams, G. *Trans. Faraday Soc.* **1966**, *62*, 132.
(35) Williams, G. *Trans. Faraday Soc.* **1966**, *62*, 209.
(36) Rössler, E. *Phys. Rev. Lett.* **1990**, *65*, 1595.
(37) Pschorn, U.; Rössler, E.; Sillescu, H.; Kaufmann, S.; Schaefer, D.; Spiess, H. W. *Macromolecules* **1991**, *24*, 398.
(38) Dhinojwala, A.; Wong, G. K.; Torkelson, J. M. *Macromolecules* **1993**, *26*, 5943.
(39) Beiner, M.; Garwe, F.; Hempel, E.; Schawe, J.; Schröter, K.; Schönhals, A.; Donth, E. *Phyics A*, in press.
(40) Garwe, F.; Beiner, M.; Hempel, E.; Schawe, J.; Schröter, K.; Schönhals, A.; Donth, E. *J. Non-Cryst. Solids*, in press.